REPORT NO.
UCB/SEMM-93/02

STRUCTURAL ENGINEERING,
MECHANICS AND MATERIALS



# A GENERALIZED VISCO-PLASTICITY MODEL AND ITS ALGORITHMIC IMPLEMENTATION

by

FERDINANDO AURICCHIO

and

ROBERT L. TAYLOR

FEB 1993

DEPARTMENT OF CIVIL ENGINEERING
UNIVERSITY OF CALIFORNIA
BERKELEY, CALIFORNIA

# A GENERALIZED VISCO-PLASTICITY MODEL AND ITS ALGORITHMIC IMPLEMENTATION

F.Auricchio R.L.Taylor
Department of Civil Engineering
University of California at Berkeley, Berkeley, CA 94720 USA

**Abstract**

In this work we present a new rate-dependent model, which has the feature of being bounded by two plasticity models. After a brief review of the continuous equations for a material with inelastic behavior governed by a von Mises (J2) yield function, including both linear isotropic and kinematic hardening mechanisms, we introduce their discrete counterpart within the framework of a return mapping algorithm. Hence, we address the new material model, called *generalized visco-plasticity*, which includes as sub-cases classical visco-plasticity, classical plasticity and generalized plasticity. We discuss both the *continuous* and the *discrete-time* version for the case of a J2 associative model. Moreover, we present its algorithmic implementation in a *return map setting* as well as the form of the discrete consistent *tangent tensor*, which guarantees quadratic convergence in a Newton iterative technique. Finally, some numerical simulations are presented to illustrate the performance of the new material model.

# 1 INTRODUCTION

Key aspects of any constitutive model are its ability to reproduce the behavior of a real material and the cost of its algorithmic implementation, which opens the possibility of numerical simulations. Relatively to the first aspect, it is well known that in many practical problems (such as dynamic loading conditions) the actual behavior of a material is governed by permanent rate-independent (plastic) effects as well as by rheological (visco) effects. Sometimes it can even happen that the rheological effects are more pronounced after the plastic state has been reached. For example, under dynamic loading many metals show a variable yield limit, increasing with the strain rate and bounded within a finite interval. Moreover, they often present a smooth change of behavior from the elastic to the plastic range. Consequently, any suitable constitutive model must be able to reproduce at least some of these important features of real material behavior, which are usually determined by experimental investigations, such as those discussed by Campbell [3], Clark [5] and Harste [6].

Looking at some of the available literature on visco-plastic theories, such as the ones discussed in Perzyna [17], Chaboche [4] and McDowell [15], it seems that the efforts to create constitutive models showing the appropriate response in terms of simulation of real material behavior are often at the expenses of the algorithmic implementation, and hence limit the possible final use of these models.

The purpose of this paper is to present a new rate dependent model, which shows some of the features mentioned above and whose algorithmic implementation is at the same time simple and straightforward. The model is called *generalized visco-plasticity*, since it includes classical visco-plasticity, classical plasticity and generalized plasticity [1, 2, 12] as sub-cases. The model has a visco-rate dependent behavior, bounded by two rate independent plasticity models; in particular it approaches either generalized plasticity or classical plasticity depending on whether the internal characteristic time is large or small compared to the loading rate. Other interesting features are: it *smoothly* reaches a limiting stress asymptote for both monotonic and cyclic loading conditions; if unloaded from the plastic range, upon reloading, it renews plasticity before the attainment of the stress where unloading began.

The discussion is organized as follow. In Section 2 we introduce the constitutive equations for a non-linear material with a von Mises (J2) yield function

and an associative flow rule. The model includes both linear isotropic and kinematic hardening mechanisms, and the capability to have a limit function different from the yield function. In Section 3 we present the discrete version of the equations introduced in Section 2, together with a brief review of the return mapping algorithm used for their integration. In Section 4 the new model and its specializations to associative plasticity for both the continuous and the discrete-time case are presented. In Section 5 and 6 we address the *tangent tensor*, consistent with the discrete model, which guarantees a quadratic convergence for a Newton iterative algorithm. In the last section we present some numerical simulations which illustrate the performance of the material model.

# 2 CONTINUOUS-TIME MODEL

We now briefly review the equations governing a material whose inelastic behavior is controlled by the second invariant of the deviatoric stress, $J_2$: we shall refer to this general class as von Mises or J2 materials. Accordingly, the evolution equations involve only the deviatoric parts of stress and strain, $\mathbf{s}$ and $\mathbf{e}$ respectively, which are related to the total stress $\boldsymbol{\sigma}$ and to the total strain $\boldsymbol{\epsilon}$ through the usual relations:

$$\begin{aligned} \boldsymbol{\sigma} &= \frac{1}{3}\mathrm{tr}(\boldsymbol{\sigma})\mathbf{1} + \mathbf{s} \\ \boldsymbol{\epsilon} &= \frac{1}{3}\mathrm{tr}(\boldsymbol{\epsilon})\mathbf{1} + \mathbf{e} \end{aligned}$$

$\mathbf{1}$ being the second order unit tensor and $\mathrm{tr}(\cdot)$ the trace operator. The linear vector space of second order tensors is equipped with the natural (Euclidean) inner product, defined by the trace of the product of any second order tensor, $\mathbf{a}$. Accordingly:

$$\|\mathbf{a}\| = [\mathbf{a} : \mathbf{a}]^{\frac{1}{2}} = [\mathrm{tr}(\mathbf{a} \cdot \mathbf{a})]^{\frac{1}{2}}$$

$$\mathbf{n} = \frac{\partial \|\mathbf{a}\|}{\partial \mathbf{a}} = \frac{\mathbf{a}}{\|\mathbf{a}\|} \quad , \quad \|\mathbf{n}\| = 1$$

and we note that: $\|\mathbf{s}\| = \sqrt{2J_2}$.

Moreover, the model is also based on the assumption of an associative flow rule and includes both linear isotropic and kinematic hardening mechanisms, which are controlled by the two constants $H_{iso}$ and $H_{kin}$, and the back stress tensor, $\boldsymbol{\alpha}$. Assuming an additive decomposition of the strain into an elastic and a plastic part, $\boldsymbol{\epsilon}^{el}$ and $\boldsymbol{\epsilon}^{p}$ respectively, denoting time as $t$ and the time derivative with a superposed dot, the governing equations are:

$$\mathbf{s}(t) = 2G\left[\mathbf{e}(t) - \mathbf{e}^{p}(t)\right] = 2G\mathbf{e}^{el}(t) \tag{2.1}$$

$$\boldsymbol{\Sigma}(t) = \mathbf{s}(t) - \boldsymbol{\alpha}(t) \tag{2.2}$$

$$f(t) = \|\boldsymbol{\Sigma}(t)\| - R(t) \tag{2.3}$$

$$g(t) = g\left(f(t), \boldsymbol{\xi}(t), \dot{\gamma}(t)\right) \tag{2.4}$$

$$\dot{\mathbf{e}}^{p}(t) = \dot{\gamma}(t)\frac{\partial f(t)}{\partial \boldsymbol{\Sigma}(t)} \tag{2.5}$$

$$\dot{\boldsymbol{\alpha}}(t) = \frac{2}{3}H_{kin}\dot{\mathbf{e}}^{p}(t) \tag{2.6}$$

$$\dot{\gamma}(t) \geq 0 \ , \ \dot{\gamma}(t)g(t) = 0 \tag{2.7}$$

where:

- Equation (2.1) is the linear elastic relation between the deviatoric stress $\mathbf{s}(t)$ and the elastic deviatoric strain $\mathbf{e}^{el}(t)$; $\mathbf{e}^{p}(t)$ is the deviatoric part of the plastic strain.

- Equation (2.2) is merely the definition of the *relative* stress $\boldsymbol{\Sigma}(t)$, where the back stress $\boldsymbol{\alpha}(t)$ physically represents the center of the yield surface, which can shift as a result of the kinematic hardening mechanism.

- Equation (2.3) is the von Mises yield function, where $R(t) = \sqrt{\frac{2}{3}}\sigma_y(t)$ is the radius of the yield surface and $\sigma_y(t)$ is the yield stress in uniaxial tension. The time dependence of $\sigma_y$ is due to an isotropic hardening mechanism, which in the simplest form is given by:

  $$\sigma_y(t) = \sigma_{y0} + H_{iso}\,\bar{e}^{p}(t) \tag{2.8}$$

  $\sigma_{y0}$ being the initial uniaxial yield stress, $H_{iso}$ the linear isotropic hardening parameter and $\bar{e}^{p}$ the equivalent plastic strain:

  $$\bar{e}^{p}(t) = \int_0^t \sqrt{\frac{2}{3}}\,\|\dot{\mathbf{e}}^{p}(t)\|\,dt \tag{2.9}$$

- Equation (2.4) is the limit function expressed in terms of the yield function $f$, a set of internal variable $\boldsymbol{\xi}(t)$ and a *rate factor* $\dot{\gamma}(t)$. The limit function embodies and models the rate dependency and the yielding properties of a material model. Observe that $g$ and $f$ are not required to coincide, although they might for some specific model, such as classical plasticity.

- Equation (2.5) is the evolution equation (flow rule) for the deviatoric plastic strain, in the framework of *associative* plasticity.

- Equation (2.6) is the simplest form of the Prager equation for the evolution of the back stress $\boldsymbol{\alpha}(t)$, $H_{kin}$ being the linear kinematic hardening parameter.

- Equations (2.7) are the Kuhn-Tucker conditions, which reduce the plastic problem to a constrained optimization problem.

Since we limit ourselves to the case of a von Mises yield function, the following equalities hold:

$$\frac{\partial f(t)}{\partial \boldsymbol{\Sigma}(t)} = \frac{\boldsymbol{\Sigma}(t)}{\|\boldsymbol{\Sigma}(t)\|} = \mathbf{n}(t) \tag{2.10}$$

where $\mathbf{n}(t)$ is the unit tensor normal to the yield function at $\boldsymbol{\Sigma}(t)$. As a result, equations (2.5) and (2.6) can be rewritten as:

$$\begin{aligned} \dot{\mathbf{e}}^p(t) &= \dot{\gamma}(t)\mathbf{n}(t) \\ \dot{\boldsymbol{\alpha}}(t) &= \frac{2}{3} H_{kin} \dot{\gamma}(t)\mathbf{n}(t) \end{aligned}$$

A more descriptive and general approach of the equations governing the behavior of an associative J2 material can be found in Reference [11].

# 3 DISCRETE-TIME MODEL AND INTEGRATION ALGORITHM

From a computational standpoint we treat the non-linear behavior of a material as a *strain driven* problem. Accordingly, the stress is obtained from the

strain history by means of an integration technique, such as a *return mapping* algorithm. In this section, we introduce a discrete version of the equations presented in Section 2 and review the resulting integration algorithm.

Let $[0,T] \subset \mathcal{R}$ be the time interval of interest and consider two time values within it, say $t_n$ and $t_{n+1} > t_n$, such that $t_{n+1}$ is the first time value of interest after $t_n$. To minimize the appearance of subscripts (to make the equations more readable), we introduce the convention:

$$\mathbf{a}_n = \mathbf{a}(t_n) \ , \quad \mathbf{a} = \mathbf{a}(t_{n+1})$$

where $\mathbf{a}$ is any generic quantity. Accordingly, in the discrete version of the equations the subscript $n$ indicates a quantity that is evaluated at time $t_n$, while no subscript indicates a quantity that is evaluated at time $t_{n+1}$.

Assuming that the solution is known at time $t_n$ and given by the state:

$$\{\mathbf{s}_n, \mathbf{e}_n, \mathbf{e}^p_n, \boldsymbol{\alpha}_n, \bar{e}^p_n\}$$

we wish to compute the solution at time $t_{n+1}$, given the total strain $\boldsymbol{\epsilon}$. Using the backward Euler integration formula for the plastic strain and the back stress flow rules, we obtain:

$$\mathbf{e}^p = \mathbf{e}^p_n + \lambda\, \mathbf{n} \tag{3.1}$$

$$\boldsymbol{\alpha} = \boldsymbol{\alpha}_n + \frac{2}{3} H_{kin}\, \lambda\, \mathbf{n} \tag{3.2}$$

where:

$$\lambda = \int_{t_n}^{t_{n+1}} \dot{\gamma}(t) dt$$

is the integrated rate factor. Equation (2.9) can now be rewritten as:

$$\bar{e}^p = \bar{e}^p_n + \sqrt{\frac{2}{3}}\lambda$$

Substitution of (3.1) into (2.1) yields:

$$\mathbf{s} = 2G\,(\mathbf{e} - \mathbf{e}^p_n) - 2G\,\lambda\,\mathbf{n} \tag{3.3}$$

while subtraction of (3.2) gives:

$$\boldsymbol{\Sigma} = \mathbf{s} - \boldsymbol{\alpha} = 2G\,(\mathbf{e} - \mathbf{e}^p_n) - \boldsymbol{\alpha}_n - \left(2G + \frac{2}{3} H_{kin}\right) \lambda\, \mathbf{n}$$

Note that $\lambda$ is an unknown quantity, computed by means of an integration algorithm, such as a return mapping procedure. Initially suggested by Maenchen and Sack [14] and Wilkins [23], the return mapping algorithm provides an efficient and robust integration scheme, based on a discrete enforcement of the limit equation. It belongs to the family of elastic-predictor plastic-corrector algorithms and, hence, is a two part algorithm. In the first part, a purely elastic *trial state* is computed; in the second, if the trial state violates the constitutive equation, a correction is computed and applied such that the final state is fully consistent with the model. The algorithm has been widely studied [16, 20, 21] as has its stability [7, 19]. It is interesting to recall that the incremental elasto-plastic initial value problem formulated as a constrained convex minimization problem is equivalent to the classical *maximum plastic dissipation* postulate. Using this analogy, the return mapping algorithm can be shown to be the closest point projection of the trial state to the limit surface $g = 0$. Therefore, besides its simplicity, the algorithm has a strong theoretical basis. Details of this analogy and theoretical discussions can be found in Reference [20]. For the particular case of associative J2 materials, the search for the closest point reduces to a radial return mapping.

We shall now discuss the two steps of the algorithm in more detail.

- *Trial state*: we assume that in the interval $[t_n, t_{n+1}]$ no plastic deformation occurs (i.e. $\mathbf{e}^p = \mathbf{e}^p_n$, which implies: $\lambda = 0$, $\boldsymbol{\alpha} = \boldsymbol{\alpha}_n$ ). As a result, we have as trial values:

$$\begin{aligned}
\lambda^{TR} &= 0 \\
\mathbf{e}^{p,TR} &= \mathbf{e}^p_n \\
\boldsymbol{\alpha}^{TR} &= \boldsymbol{\alpha}_n \\
\mathbf{s}^{TR} &= 2G(\mathbf{e} - \mathbf{e}^p_n) \\
\boldsymbol{\Sigma}^{TR} &= \mathbf{s}^{TR} - \boldsymbol{\alpha}^{TR} = \mathbf{s}^{TR} - \boldsymbol{\alpha}_n \\
\bar{e}^{p,TR} &= \bar{e}^p_n
\end{aligned}$$

  If the elastic trial state is admissible, i.e. it does not violate the condition $g \leq 0$, then it represents the new solution at $t_{n+1}$ and the second part of the algorithm is skipped.

- *Plastic correction*: if the trial state is not admissible, a correction has to be performed. Enforcing the condition $g = 0$, the integrated rate

factor $\lambda$ may be computed, as shown in Section 4 for the generalized visco-plasticity model. All the equations can be now rewritten in terms of the trial state and $\lambda$:

$$\begin{aligned}
\mathbf{e}^p &= \mathbf{e}^{p,TR} + \lambda\, \mathbf{n} \\
\boldsymbol{\alpha} &= \boldsymbol{\alpha}^{TR} + \frac{2}{3} H_{kin}\, \lambda\, \mathbf{n} \\
\mathbf{s} &= \mathbf{s}^{TR} - 2G\, \lambda\, \mathbf{n} \\
\boldsymbol{\Sigma} &= \boldsymbol{\Sigma}^{TR} - \left(2G + \frac{2}{3} H_{kin}\right) \lambda\, \mathbf{n} \\
\bar{e}^p &= \bar{e}^{p,TR} + \sqrt{\frac{2}{3}}\lambda
\end{aligned}$$

which allow us to compute and update the solution.

Using equation (2.10) ($\boldsymbol{\Sigma} = \|\boldsymbol{\Sigma}\|\, \mathbf{n}$) in the equation for $\boldsymbol{\Sigma}$, we deduce that $\boldsymbol{\Sigma}^{TR}$ and $\boldsymbol{\Sigma}$ have the same direction $\mathbf{n}$ (i.e. $\mathbf{n}^{TR} = \mathbf{n}$ ). Hence, a scalar relation between their norms can be derived:

$$\|\boldsymbol{\Sigma}\| = \|\boldsymbol{\Sigma}^{TR}\| - \left(2G + \frac{2}{3} H_{kin}\right) \lambda$$

and a radial return can be performed. Note that, once $\lambda$ is determined, the state $\{\mathbf{s}, \mathbf{e}, \mathbf{e}^p, \boldsymbol{\alpha}, \bar{e}^p\}$ may be easily computed.

# 4 THE GENERALIZED VISCO-PLASTICITY MODEL

We first introduce a new generalized visco-plasticity model in its continuous version and consider its specialization to the case of J2 associative plasticity. Then we address the discrete version of the model, which we treat within the framework of the return mapping algorithm, outlined in the previous section.

## 4.1 The continuous-time model

A simple model of generalized plasticity was introduced in Reference [12] and its numerical implementation was discussed in References [1] and [2].

Referring to the notation of these works, the limit function of the visco-plastic model is:

$$g = \alpha_1 h\,[\mathbf{n}^* : \dot{\boldsymbol{\sigma}}] + \frac{\alpha_2}{\tau}\Phi\left(\frac{f}{R_o}\right) - \alpha_3\dot{\gamma} \tag{4.1}$$

where: the $\alpha_i$ $(i = 1, 2, 3)$ are constants which may be set equal to 1 or 0 to render active or inactive each term of the model, $\mathbf{n}^* = \partial f/\partial\boldsymbol{\sigma}$ is the normal to the yield function $f$, $\tau$ is an internal characteristic time parameter, $\Phi$ is a function deduced from dynamic tests on the material, $R_o = \sqrt{\frac{2}{3}}\sigma_o$ is the initial radius of the yield surface and $h$ is a non-linear function of $f$. We assume:

$$h = \frac{f}{\delta(\beta - f) + \frac{2}{3}H\beta}$$

with $\beta$ and $\delta$ two positive parameters with dimensions of stress and $H = H_{iso} + H_{kin}$. In particular $\beta$ is a scalar measure of the distance between the asymptotic and the initial radius of the yield function, while $\delta$ measures the speed of the model in approaching the asymptotic behavior. Using the relations:

$$\beta = \sqrt{\frac{2}{3}}\beta_u \quad , \quad \delta = \frac{2}{3}\delta_u$$

$\beta$ and $\delta$ can be related to the corresponding parameters computed in a one-dimensional setting, which means that now $\beta_u$ measures the distance between the asymptotic stress and the yield stress $\sigma_y$ and $\delta_u$ measures the speed of the model in approaching the asymptotic behavior.

From equation (4.1), it is possible to check that the limiting behaviors of the model are two rate independent plasticity models. For values of the internal characteristic time $\tau$ which are large compared to the loading rate $p$ the viscous part, i.e. the one associated with $\alpha_2$, drops out and the model reduces to the generalized plasticity model, described in References [1, 2, 12]. For small values of the internal time $\tau$, again compared to the loading rate $p$, the viscous effects are large and make negligible the part of the response associated with $\alpha_1$ and $\alpha_3$, hence the model reduces to classical plasticity. It is also interesting to point out how several different simpler models can be

| Model | $\alpha_1$ | $\alpha_2$ | $\alpha_3$ |
|---|---|---|---|
| Classical visco-plasticity | 0 | 1 | 1 |
| Generalized plasticity | 1 | 0 | 1 |
| Classical plasticity | 0 | 1 | 0 |
| Classical plasticity ($\beta_u = 0$) | 1 | 0 | 1 |

Table 1: Possibility of retrieving simpler models with appropriate choice of the $\alpha$ parameters

directly retrieved with particular choices of the $\alpha$ parameters, according to Table 1.

The model so far discussed resembles in part the one proposed by Lubliner in References [9, 10], which is however obtained by a different approach and discussed only in a one-dimensional setting.

We now consider how the model specializes in the case of associative J2 plasticity, for which the term $(\mathbf{n}^* : \dot{\boldsymbol{\sigma}})$ can be expressed in a more explicit form. Accordingly, treating $\boldsymbol{\alpha}$ as a dependent variable, we have:

$$\mathbf{n}^* = \frac{\partial f}{\partial \boldsymbol{\Sigma}} \frac{\partial \boldsymbol{\Sigma}}{\partial \boldsymbol{\sigma}} = \mathbf{n} \frac{\partial \mathbf{s}}{\partial \boldsymbol{\sigma}} = \mathbf{n}$$

Therefore:

$$\mathbf{n}^* : \dot{\boldsymbol{\sigma}} = \mathbf{n} : \dot{\mathbf{s}} = \mathbf{n} : \dot{\boldsymbol{\Sigma}} + \mathbf{n} : \dot{\boldsymbol{\alpha}} = \mathbf{n} : \dot{\boldsymbol{\Sigma}} + \frac{2}{3}\dot{\gamma} H_{kin} \tag{4.2}$$

Noting that:

$$\mathbf{n} : \mathbf{n} = 1 \quad \Rightarrow \quad \mathbf{n} : \dot{\mathbf{n}} = \dot{\mathbf{n}} : \mathbf{n} = 0$$

equation (4.2) simplifies:

$$\mathbf{n}^* : \dot{\boldsymbol{\sigma}} = \mathbf{n} : \frac{d}{dt}(\|\boldsymbol{\Sigma}\|\mathbf{n}) + \frac{2}{3}\dot{\gamma} H_{kin} = \frac{d}{dt}\|\boldsymbol{\Sigma}\| + \frac{2}{3}\dot{\gamma} H_{kin}$$

As a result, the limit function (4.1) can be rewritten as:

$$g = \alpha_1 h \left[ \frac{d}{dt}\|\boldsymbol{\Sigma}\| + \frac{2}{3}\dot{\gamma} H_{kin} \right] + \frac{\alpha_2}{\tau} \Phi \left( \frac{f}{R_o} \right) - \alpha_3 \dot{\gamma} \tag{4.3}$$

## 4.2 The discrete-time model

We now present the discrete version of the J2 associative generalized visco-plasticity model, previously addressed in its continuous form. The discrete model is required to properly evaluate the integrated rate factor $\lambda$ for the solution of a discrete-time problem. Since $\lambda$ may be interpreted as a measure of the correction that renders admissible a non-admissible trial state, it must be computed enforcing the condition $g = 0$ in a discrete-time setting. We assume $\Phi(f) = f^2$, often adopted for metal plasticity [17].

Integrating the condition $g = 0$ over the time interval $[t_n, t_{n+1}]$, we obtain:

$$\alpha_1 h \left[ \|\boldsymbol{\Sigma}\| - \|\boldsymbol{\Sigma}_n\| + \frac{2}{3}\lambda\, H_{kin} \right] + \alpha_2 \frac{\Delta t}{\tau} \left( \frac{f}{R_o} \right)^2 - \alpha_3 \lambda = 0 \tag{4.4}$$

If we set:

$$\begin{aligned} A_1 &= \|\boldsymbol{\Sigma}^{TR}\| - R_n \\ A_2 &= \|\boldsymbol{\Sigma}^{TR}\| - \|\boldsymbol{\Sigma}_n\| \\ A_3 &= -\left(\delta + \frac{2}{3}H\right)\beta \\ A_4 &= \frac{\Delta t}{\tau R_o^2} \end{aligned}$$

after clearing fractions, the limit equation can be rewritten as:

$$\alpha_1 f \left[ A_2 - 2G\lambda \right] - \alpha_2 A_4 f^2 \left[ A_3 + \delta f \right] + \alpha_3 \lambda \left[ A_3 + \delta f \right] = 0$$

Recalling the scalar relation between $\|\boldsymbol{\Sigma}^{TR}\|$ and $\|\boldsymbol{\Sigma}\|$ and the definition of $R$, we have:

$$\begin{aligned} f &= \|\boldsymbol{\Sigma}\| - R \\ &= \left[ \|\boldsymbol{\Sigma}^{TR}\| - \left(2G + \frac{2}{3}H_{kin}\right)\lambda \right] - \left(R_n + \frac{2}{3}H_{iso}\lambda\right) \\ &= A_1 - 2G_1\lambda \end{aligned}$$

where:

$$G_1 = G + \frac{1}{3}\left(H_{iso} + H_{kin}\right)$$

Eventually, performing some algebraic manipulations, we end up with the following cubic equation in $\lambda$:

$$c_1\lambda^3 + c_2\lambda^2 + c_3\lambda + c_4 = 0 \tag{4.5}$$

where:

$$\begin{array}{rcccc} c_1 & = & & \alpha_2\left[8G_1^3\delta A_4\right] & \\ c_2 & = & \alpha_1\left[4GG_1\right] & -\alpha_2 A_4 4G_1^2\left[3\delta A_1 + A_3\right] & -\alpha_3 2G_1\delta \\ c_3 & = & \alpha_1\left[2GA_1 + 2G_1A_2\right] & +\alpha_2 2G_1A_1A_4\left[3\delta A_1 + 2A_3\right] & +\alpha_3\left[A_1\delta + A_3\right] \\ c_4 & = & +\alpha_1 A_1A_2 & -\alpha_2 A_1^2A_4\left[\delta A_1 + A_3\right] & \end{array}$$

The roots can be computed in closed form as discussed in Reference [18]. It is interesting to observe that, starting from the cubic equation (4.5) and with the choice of the $\alpha$ parameters set in Table 1, it is possible to derive in closed form the integrated rate factor for simpler material models such as classical visco-plasticity, classical plasticity and generalized plasticity.

Finally, observe that in the generalized visco-plasticity model an admissible inelastic state of stress can be outside the surface $f$; but it must always be on the surface $g$ (i.e. $g = 0$). Since the return mapping algorithm is such that the trial state is projected on the limit equation surface, the condition $g^{TR} > 0$ is sufficient to determine if a step is plastic.

# 5 CONSISTENT ALGORITHMIC TANGENT TENSOR

We now address the form of the tangent tensor, consistent with the discrete J2 associative plasticity model described in Section 3. In the next section, we then specialize the form of the tensor to the generalized plasticity model. The use of the tangent moduli preserves the quadratic convergence of a Newton method, which we adopt in Section 7 for the incremental solution of a finite element scheme.

We start by linearizing equations (3.3) and (3.2) about a solution point:

$$d\mathbf{s} = 2Gd\mathbf{e} - 2G\mathbf{n}d\lambda - 2G\lambda d\mathbf{n} \tag{5.1}$$

$$d\boldsymbol{\alpha} = \frac{2}{3}H_{kin}\mathbf{n}d\lambda + \frac{2}{3}H_{kin}\lambda d\mathbf{n} \tag{5.2}$$

If we assume that the linearization of the limit equation yields an expression of the type:

$$d\lambda = A\,(\mathbf{n} : d\mathbf{e})$$

we can solve equations (5.1) and (5.2) for $d\mathbf{s}$:

$$d\mathbf{s} = 2G\,[(1-C)\mathbf{I} + (C-A)\,(\mathbf{n}\otimes\mathbf{n})]\,d\mathbf{e}$$

where:

$$C = \frac{2G\lambda}{\|\boldsymbol{\Sigma}^{TR}\|}$$

This is an incremental relation between the deviatoric part of the stress tensor $\mathbf{s}$ and the deviatoric part of the strain tensor $\mathbf{e}$, consistent with the discrete J2 associative plasticity model of Section 3. Under the assumption of linear elasticity, we can get an incremental relation between the total stress tensor $\boldsymbol{\sigma}$ and the total strain tensor $\boldsymbol{\epsilon}$ :

$$d\boldsymbol{\sigma} = \mathbf{D}^{ep} d\boldsymbol{\epsilon}$$

where the algorithmic elastic-inelastic tangent tensor is finally given by:

$$\mathbf{D}^{ep} = [K\,(\mathbf{1}\otimes\mathbf{1}) + 2G\,(1-C)\,\mathbf{I}_{dev} + 2G\,(C-A)\,(\mathbf{n}\otimes\mathbf{n})] \tag{5.3}$$

in which $K$ is the bulk modulus and $\mathbf{I}_{dev}$ is a rank four tensor defined as:

$$\mathbf{I}_{dev} = \mathbf{I} - \frac{1}{3}(\mathbf{1}\otimes\mathbf{1})$$

A more detailed discussion on the construction of the tangent tensor for material models for which $d\lambda = A\,(\mathbf{n} : d\mathbf{e})$ holds can be found in References [1] and [2].

# 6 CONSISTENT DISCRETE TANGENT TENSOR FOR THE GENERALIZED VISCO-PLASTICITY MODEL

In Section 5 we presented a form of the tangent tensor, consistent with the discrete J2 associative plasticity model of Section 3 and involving a coefficient $A$ coming from the linearization of the discrete limit equation. In the

following, we compute this scalar factor for the generalized visco-plasticity model.

Noting that:

$$\begin{aligned} d\|\boldsymbol{\Sigma}\| &= 2G\,(\mathbf{n} : d\mathbf{e}) - \left(2G + \frac{2}{3}H_{kin}d\lambda\right) \\ df &= d\|\boldsymbol{\Sigma}\| - dR = 2G\,(\mathbf{n} : d\mathbf{e}) - 2G_1 d\lambda \end{aligned}$$

we can linearize the discrete limit equation (4.4) and obtain a relation of the form:

$$d\lambda = A\,(\mathbf{n} : d\mathbf{e})$$

where:

$$A = \frac{2G\left\{\alpha_1\left[D_1 + D_2\right] + \alpha_2\left[D_2 D_3 D_4\right] + \alpha_3\left[\delta\lambda\right]\right\}}{\alpha_1\left[2G_1 D_1 + 2GD_2\right] + \alpha_2\left[2G_1 D_2 D_3 D_4\right] + \alpha_3\left[2G_1\lambda\delta + D_5\right]} \tag{6.1}$$

with:

$$\begin{aligned} D_1 &= \|\boldsymbol{\Sigma}\| - \|\boldsymbol{\Sigma}_n\| + \frac{2}{3}H_{kin}\lambda \\ D_2 &= \|\boldsymbol{\Sigma}\| - \left(R_n + \frac{2}{3}H_{iso}\lambda\right) = f \\ D_3 &= 2\left(\delta + \frac{2}{3}H\right)\beta - 3D_2\delta \\ D_4 &= \frac{\Delta t}{\tau R_o^2} \\ D_5 &= \delta\,(\beta - f) + \frac{2}{3}H\beta \end{aligned}$$

Note that starting from equation (6.1) and with a proper choice of the $\alpha$ parameters, it is possible to retrieve the correct form of the factor $A$ for simpler material models, such as classical visco-plasticity, classical plasticity or generalized plasticity.

# 7 NUMERICAL EXAMPLES

In this section we present some numerical examples performed to test the generalized visco-plasticity model. They are all obtained running a three

dimensional finite element, based on a *mixed* approach [22] and implemented into the Finite Element Analysis Program (FEAP) [24, 25].

The numerical simulations are organized as follow:

- Uniaxial tension test: rate dependent effects
- Uniaxial tension test: reduction to simpler model
- Uniaxial tension test: cyclic load
- Thin walled tube in tension and torsion

In all the examples we consider a cubic specimen of side length equal to 10, with boundary and loading conditions set to produce the appropriate stress state. The load is usually applied controlling the displacements. The sample is modeled with only one element and the material properties are:

$$E = 100 \ , \quad \nu = 0.3 \ , \quad H_{iso} = H_{kin} = 0$$

## 7.1 Uniaxial tension test: rate dependent effects

The material properties are:

$$\sigma_y = 15 \ , \quad \beta_u = 10 \ , \quad \delta_u = 20$$

In a first group of analyses, we test the model for different values of the internal characteristic time $\tau$ and fixed loading rate $p$; in particular, we used $\tau \in \{0.01, 1, 100\}$ and $p = 1$. In fig.1 the stress-strain curves are reported together with the generalized plasticity and the classical plasticity solutions. We can observe that for high values of $\tau$ the generalized visco-plasticity model tends to generalized plasticity (for $\tau = 100$ the two solutions almost coincide), while for low values of $\tau$ it tends to classical plasticity.

In a second group of analyses we fix the value of the internal characteristic time $\tau$ and vary the loading rate $p$; in particular we used $\tau = 100$ and $p \in \{10, 100, 1000\}$. In fig.2 the stress-time curves are reported; in terms of stress-strain similar results of those presented in fig.1 are recovered, as should be expected.

## 7.2 Uniaxial tension test: reduction to simpler model

The capacity of the generalized visco-plasticity model to reduce to simpler material models by a correct choice of the $\alpha$ parameters has also been tested numerically, in order to check any instability or numerical problem.

All the simpler models have been reproduced perfectly. In particular the generalized plasticity model retains all its characteristics, such as:

- after initial yield, it shows a smooth transition before reaching an asymptote,
- if unloaded from the plastic range, upon reloading, it renews plasticity before the attainment of the stress where unloading began,
- the asymptote is approached faster for larger values of $\delta_u$.

## 7.3 Uniaxial tension test: cyclic load

This time the specimen undergoes a cyclic uniaxial load history presented in fig.3. The load history has some periodic time-interval of constant load, to check the relaxation of the model as suggested for rate dependent model in Reference [8]. The material properties are:

$$\sigma_y = 15 \ , \quad \beta_u = 10 \ , \quad \delta_u = 20$$

The axial stress is plotted versus the axial strain in fig.4. Observe that the generalized visco-plasticity material model retains all its properties also under cyclic loading; moreover, the relaxation effect depends on the value of the internal characteristic time $\tau$, which means that for high value of $\tau$ (materials requiring a *long* time to respond to a change of the external load conditions) the length of constant load time-interval is too short for the model to feel it.

## 7.4 Thin walled tube in tension and torsion

We consider a thin walled circular tube with inner and outer radii equal to 9.75 and 10.25, respectively. The material properties are:

$$\sigma_y = 10 \ , \quad \beta_u = 5 \ , \quad \delta_u = 30$$

By controlling the displacements, the tube is initially pulled in tension beyond the yielding limit (i.e. up to a value of axial deformation equal to 1) and then a tangential displacement (torsion) is applied, leaving the axial displacement unchanged (fig.5). The axial and the tangential stresses are plotted versus time in figs.6 and 7 for different values of the internal characteristic time $\tau$. Note that, as the shear stress approaches the limiting value, the axial stress approaches zero and a virtually pure torsion is attained for all values of $\tau$. Hence, the elastic part of the constant axial strain changes from purely elastic to plastic, as the tangential displacement is increased.

# 8 CLOSURE AND FURTHER DIRECTIONS OF RESEARCH

In this work we introduced and discussed a new generalized visco-plasticity model, which includes as sub-cases generalized plasticity [1, 2, 12], classical plasticity [11] and classical visco-plasticity [17]. We present also the algorithmic implementation of the model as a return mapping algorithm. For applications using the finite element method and a Newton iterative solution technique, we also address the algorithmic tangent tensor consistent with the discrete-time model. All of the development includes both isotropic and kinematic hardening.

Solutions to example problems illustrate some interesting features of the model; in particular it has the property of having two plasticity models as limiting behavior: it tends to generalized plasticity or to classical plasticity depending if the ratio of the loading rate $p$ and the internal characteristic time $\tau$ is large or small. Moreover, the model retains all the feature of the generalized plasticity: it *smoothly* reaches a limiting asymptote for both monotonic and cyclic loading conditions; if unloaded in the plastic range, upon reloading, it renews plasticity before the attainment of the stress where unloading began.

We note that the generalized visco-plasticity model may be implemented into existing finite element programs, originally limited to classical plasticity alone, with only minor modification and extension. Namely, the appropriate limit equation and tangent factor $A$ must be specialized for the model.

Finally, we want to stress that the model can be easily extended to pro-

duce more realistic responses. For example, as pointed out by Lubliner [13], in equation (4.1) the function $f$ appearing in the nonlinear function $h$ can be different from the function $f$ used as the argument of $\Phi$. In the future the authors plan to extend the model in this direction as well as to introduce the possibility of a generalized visco-plasticity model, whose limiting behavior are two different generalized plasticity model.

## Acknowledgement

The authors would like to acknowledge Professor J.Lubliner for many useful discussions on the generalized plasticity model and for his suggestions relatively to the generalized visco-plasticity model.

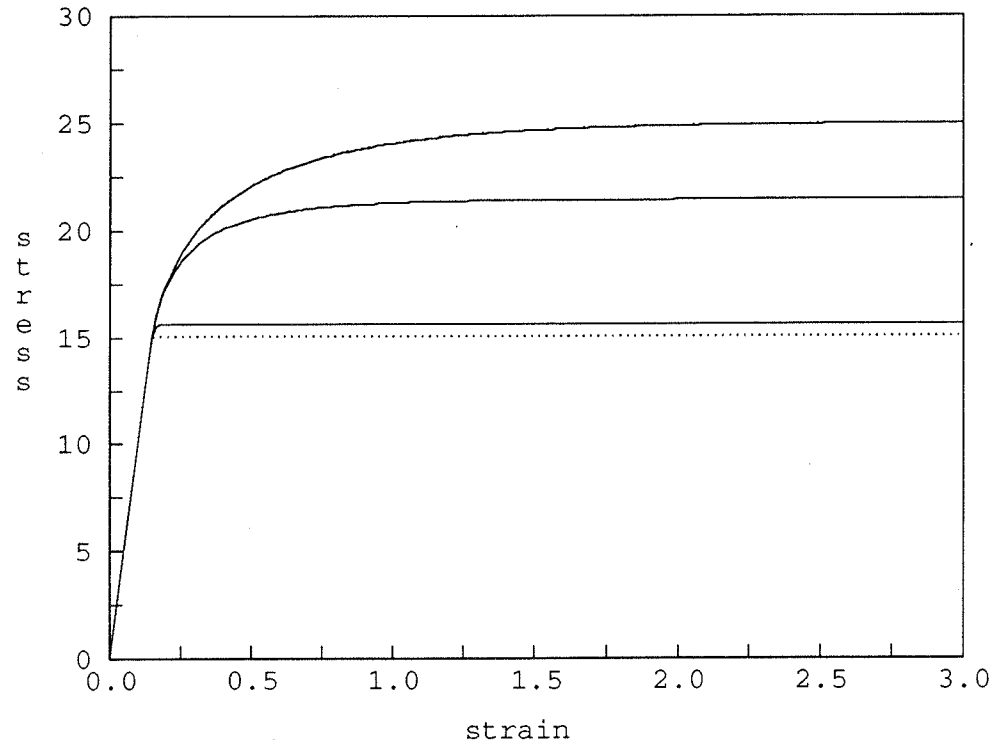


Figure 1: Uniaxial tension test: rate dependent effects. Dependence on the characteristic time: stress versus strain.
$\sigma_y = 15$ , $\beta = 10$ , $\delta = 20$ , $H_{iso} = H_{kin} = 0$. Loading rate $p = 1 = \text{const}$, characteristic time $\tau \in \{0.01, 1, 100\}$. The solution for the classical plasticity and the generalized plasticity models are reported with dotted lines. The latter almost overlaps the solution for $\tau = 100$.

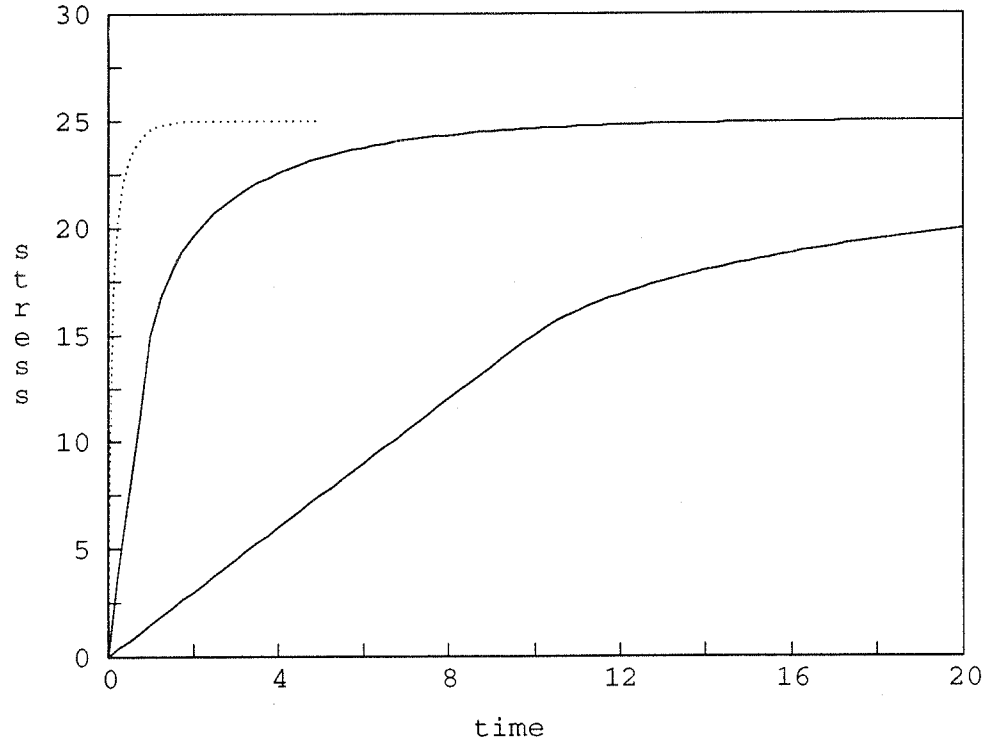


Figure 2: Uniaxial tension test: rate dependent effects. Dependence on the loading rate: stress versus time.
$\sigma_y = 15$ , $\beta = 10$ , $\delta = 20$ , $H_{iso} = H_{kin} = 0$. Loading rate $p \in \{10, 100, 1000\}$, characteristic time $\tau = 100 = \text{const}$. The solution for $p = 1000$ is reported with a dotted line.

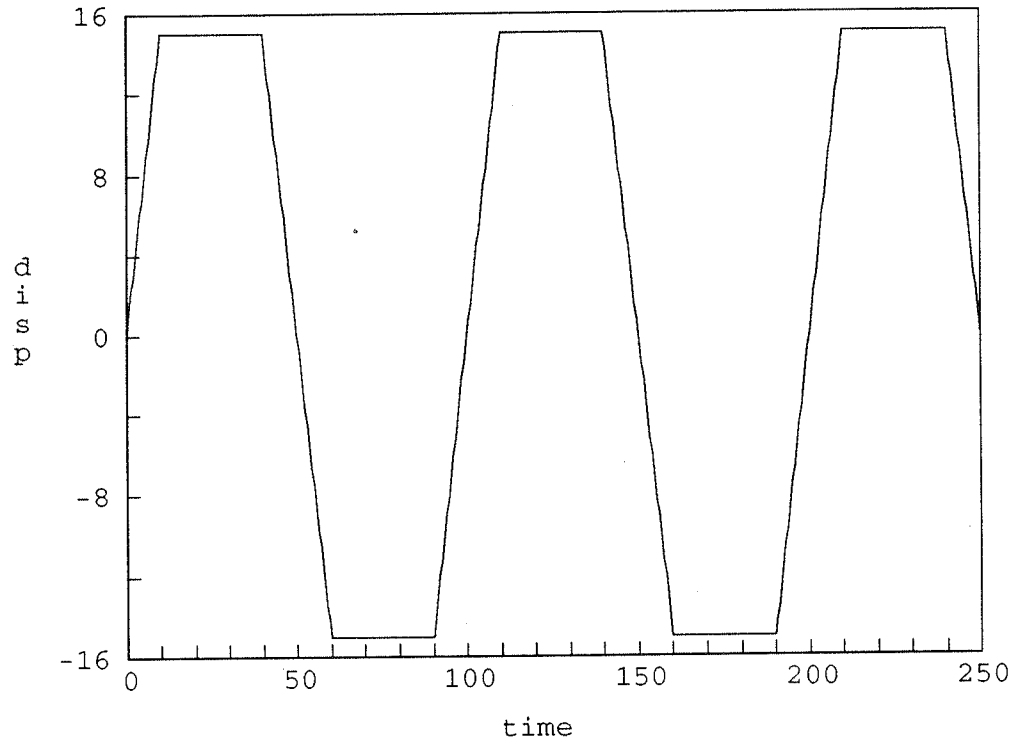


Figure 3: Uniaxial tension test: cyclic loading. Time history: displacement versus time.

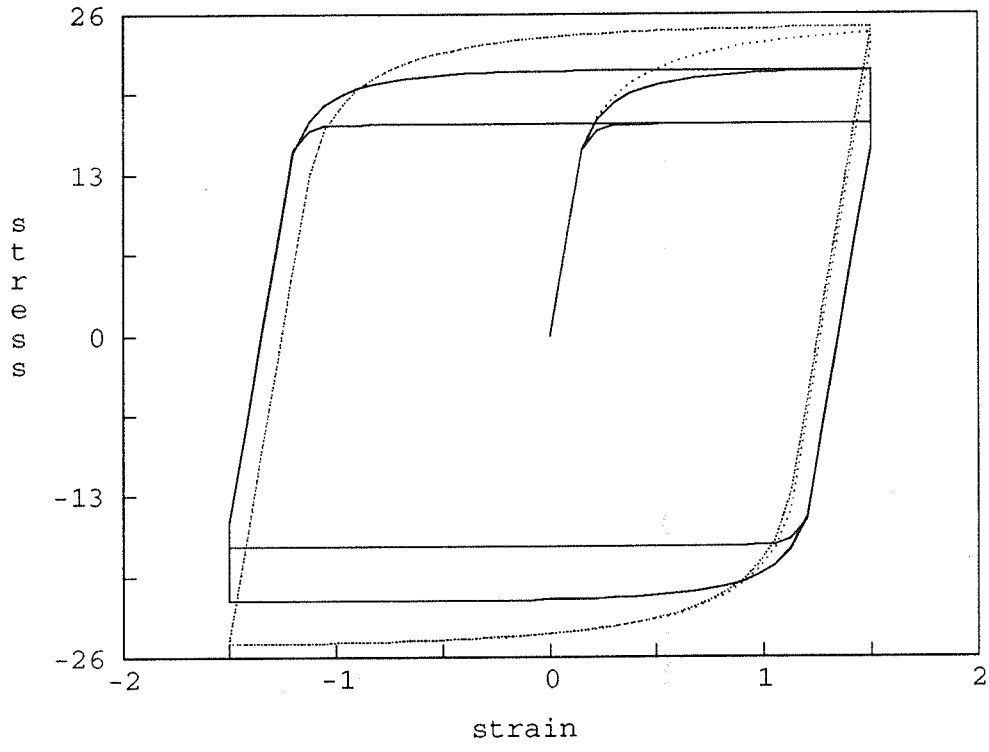


Figure 4: Uniaxial tension test: cyclic loading. Stress versus time.
$\sigma_y = 15$ , $\beta = 10$ , $\delta = 20$ , $H_{iso} = H_{kin} = 0$. Loading rate $p = 1 = \text{const}$, characteristic time $\tau \in \{0.1, 1, 10\}$. The solution for $\tau = 10$ is reported with a dotted line.

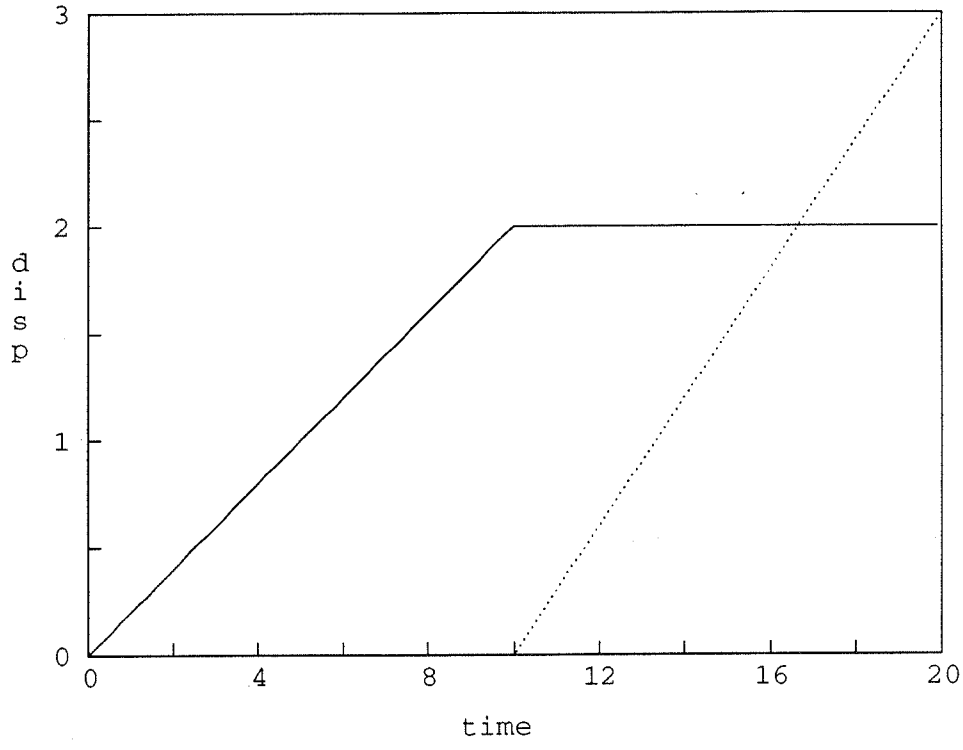


Figure 5: Thin walled tube in tension and torsion.
Time history: normal and tangential displacements versus time. The tangential displacement is reported with a dotted line.

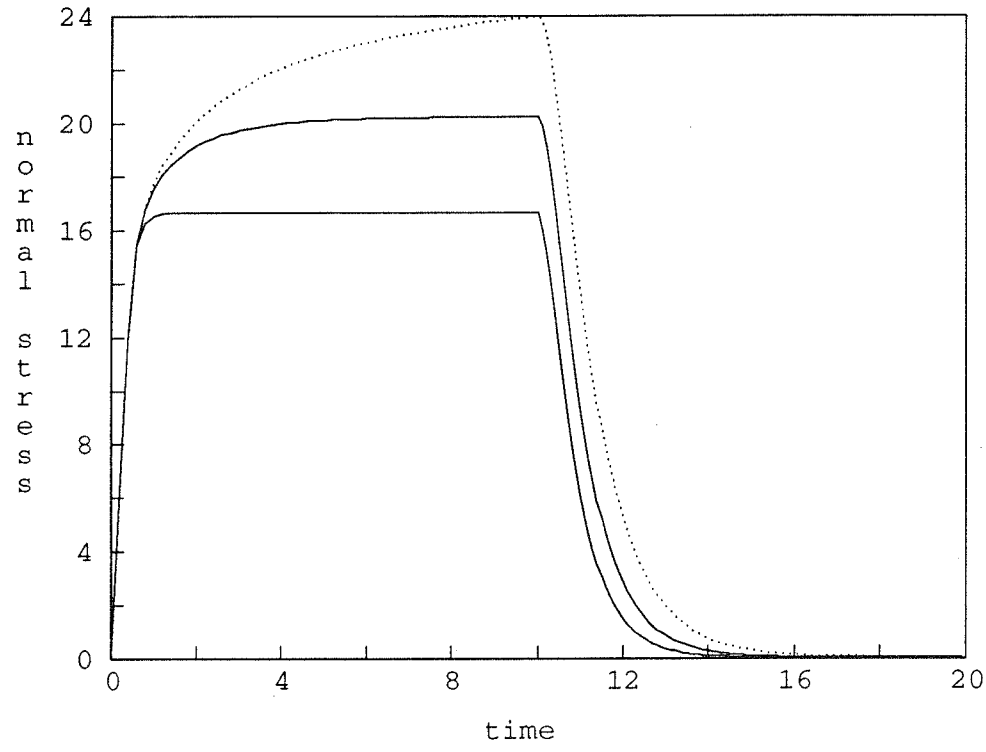


Figure 6: Thin walled tube in tension and torsion. Normal stress $\sigma_{zz}$ versus time.
Loading rate $p = 1 = \text{const}$, characteristic time $\tau \in \{0.1, 1, 10\}$. The solution for $\tau = 10$ is reported with a dotted line.

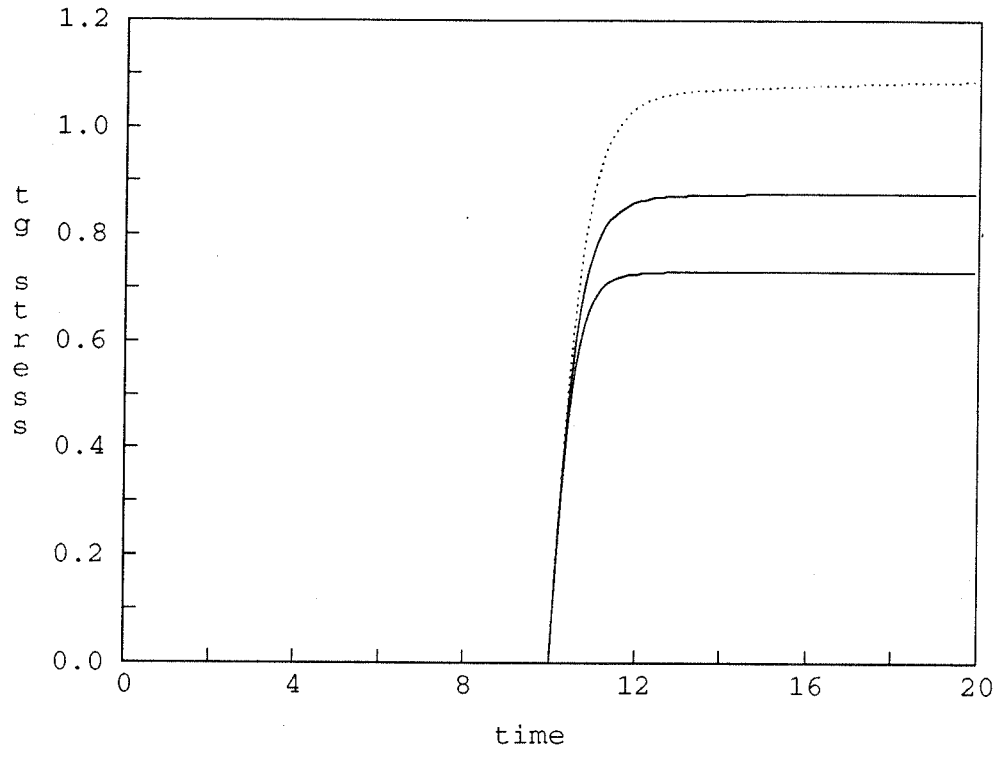


Figure 7: Thin walled tube in tension and torsion. Tangential stress $\sigma_{z\theta}$ versus time.
Loading rate $p = 1 = \text{const}$, characteristic time $\tau \in \{0.1, 1, 10\}$. The solution for $\tau = 10$ is reported with a dotted line.

# References

[1] F. Auricchio and R.L. Taylor, *Two material models for cyclic plasticity: non-linear kinematic hardening and generalized plasticity*, submitted for publication.

[2] F. Auricchio, R.L. Taylor, and J. Lubliner, *Application of a return map algorithm to plasticity models*, COMPLAS Computational Plasticity: Fundamentals and Applications (Barcelona) (D.R.J. Owen and E. Onate, eds.), 1992, pp. 2229–2248.

[3] J.D. Campbell, *The dynamic yielding of mild steel*, Acta Metallurgica **1** (1953), 706–710.

[4] J.L. Chaboche, *Constitutive equations for cyclic plasticity and cyclic visco-plasticity*, International Journal of Plasticity **5** (1989), 247–302.

[5] D.S. Clark, *The behavior of metals under dynamic loading*, Transaction of the American Society for Metals **46** (1954), 32–62.

[6] K. Harste, T. Suzuki, and K. Schwerdtfeger, *Thermomechanical properties of steel: viscoplasticity of $\gamma$ iron and $\gamma$ Fe-C alloys*, Materials Science and Technology **8** (1992), 23–32.

[7] R.D. Krieg and D.B. Krieg, *Accuracies of numerical solution methods for the elastic-perfectly plastic model*, Journal of Pressure Vessel Technology, Transaction of ASME (1977), 510–515.

[8] J. Lemaitre and J.L. Chaboche, *Mechanics of solid materials*, Cambridge University Press, 1990.

[9] J. Lubliner, *A generalized theory of strain-rate-dependent plastic wave propagation in bars*, Journal of the Mechanics and Physics of Solids **12** (1964), 59–65.

[10] ———, *The strain-rate effect in plastic wave propagation*, Journal de Mecanique **4** (1965), 111–120.

[11] ———, *Plasticity theory*, Macmillan, 1990.

[12] ———, *A simple model of generalized plasticity*, International Journal of Solids and Structures **28** (1991), 769–778.

[13] ———, Private Communication, 1993.

[14] G. Maenchen and S. Sack, *The tensor code*, Methods in computational physics (B. Alder, ed.), vol. 3, Academic Press, 1964, pp. 181–210.

[15] D.L. McDowell, *A non-linear kinematic hardening theory for cyclic thermo-plasticity and thermo-visco-plasticity*, International Journal of Plasticity **8** (1992), 695–728.

[16] J.C. Nagtegaal, *On the implementation of inelastic constitutive equations with special reference to large deformation problems*, Computer Methods in Applied Mechanics and Engineering **33** (1982), 469–484.

[17] P. Perzyna, *Fundamental problems in viscoplasticity*, Advances in Applied Mechanics, vol. 9, Academic Press, 1966, pp. 243–377.

[18] W.H. Press, B.P. Flannery, S.A. Teukolsky, and W.T. Vetterliy, *Numerical recipes in C: the art of computing*, Cambridge University Press, 1988.

[19] J.C. Simo and S. Govindjee, *Non-linear B-stability and symmetry preserving return mapping algorithms for plasticity and visco-plasticity*, International Journal for Numerical Methods in Engineering **31** (1991), 151–176.

[20] J.C. Simo and T.J.R. Hughes, *Elasto-plasticity and visco-plasticity: computational aspects*, Springer-Verlag, 1993, to be published.

[21] J.C. Simo and R.L. Taylor, *Consistent tangent operators for rate-independent elasto-plasticity*, Computer Methods in Applied Mechanics and Engineering **48** (1985), 101–118.

[22] J.C. Simo, R.L. Taylor, and K.S. Pister, *Variational and projection methods for the volume constraint in finite deformation elasto-plasticity*, Computer Methods in Applied Mechanics and Engineering **51** (1985), 177–208.

[23] M.L. Wilkins, *Calculation of elastic plastic flow*, Methods in computational physics (B. Alder, ed.), vol. 3, Academic Press, 1964, pp. 211–263.

[24] O.C. Zienkiewicz and R.L. Taylor, *The finite element method*, fourth ed., vol. I, McGraw Hill, New York, 1989.

[25] ———, *The finite element method*, fourth ed., vol. II, McGraw Hill, New York, 1991.

# List of Tables

# List of Figures